NANO LETTERS
Cite This: Nano Lett. 2018, 18, 6764−6769
Letter
pubs.acs.org/NanoLett

Andreev Reflection in a Superconducting Light-Emitting Diode

Dmitry Panna, Shlomi Bouscher, Krishna Balasubramanian, Vicky Perepelook, Shimon Cohen, Dan Ritter, and Alex Hayat*

Department of Electrical Engineering, Technion, Haifa 32000, Israel

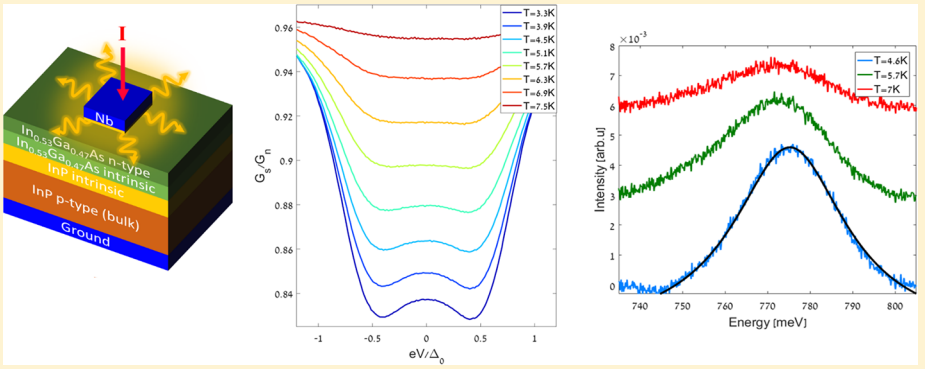

ABSTRACT: We experimentally demonstrate Cooper-pair injection into a superconducting light-emitting diode by observing Andreev reflection at the superconductor−semiconductor interface, overcoming the contradicting requirements of an electrically transparent interface and radiative recombination efficiency. The device exhibits electroluminescence enhancement at the quasi-Fermi energy at temperatures below T_c. The theoretically predicted conductance and electroluminescence spectra based on Cooper-pair injection into the semiconductor correspond well to our experimental results. Our findings pave the way for practical superconductor−semiconductor quantum light sources.

KEYWORDS: *Superconductors, semiconductors, LED, Andreev reflection*

Hybrid superconductor−semiconductor devices are a rapidly growing field of research, with a wide range of applications, including a variety of quantum devices,[1−10] such as quantum dot (QD) based light-emitting diodes (LEDs),[4−6] Bell-state analyzers,[8] and superconducting two-photon amplifiers.[9] One of the most promising directions in these hybrid devices is generation of entangled-photon pairs[11] through Cooper-pair luminescence[12] in compact semiconductor devices, crucial for practical quantum technologies. Non-superconducting semiconductor sources of entangled photon pairs have been demonstrated previously, based on optically excited QD biexciton decay,[13] although with limited emission rates due to the isolated QD single emitter. Photon-pair emission was also shown in semiconductors by electrically driven two-photon emission[14,15] suitable for entanglement generation.[16] However, it has been shown that two-photon emission is weaker by 5 orders of magnitude than one-photon emission, requiring sophisticated photonic enhancement approaches.[17−19]

Sources of entangled photons based on superconductor−semiconductor structures offer high-rate photon pair generation in miniaturized electrically pumped devices.[11] Moreover, unlike QDs they do not require isolated emitters due to the fundamentally different origin of the photon entanglement. In contrast to the Pauli exclusion principle in QDs with discrete energy levels, the origin of photon entanglement in superconducting devices is the electron entanglement in Cooper-pairs.[20] This electron entanglement can be transferred to emitted photon-pair entanglement, when Cooper-pairs are injected from a superconductor into a semiconductor light emitting structure, such as QDs employing discrete energy levels,[5] as well as in quantum-wells with energy continuum.[11]

Cooper-pair injection into the normal material can be detected experimentally through the phenomenon of Andreev reflection[21] appearing as enhancement of conductance within the vicinity of the superconducting gap, a zero-bias conductance peak (ZBCP).[22] Several superconducting LED (SLED) devices have been studied in the past[3−5,7,23,24] demonstrating Josephson effects and enhanced light emission. While Josephson effects are interesting and promising for future superconducting optoelectronics,[25−28] they occur in a wide range of superconductor-normal metal or superconductor−insulator junctions, (including vacuum as an insulator) and thus do not exhibit unique signatures of Cooper pair injection into the semiconductor. Nevertheless, direct demonstration of Cooper-pair injection into light emitting structures by Andreev reflection has not been achieved before.

Here we present the first direct experimental demonstration of Cooper-pair injection into a light-emitting structure by showing Andreev reflection at the superconductor−semicon-

Received: June 20, 2018
Revised: October 9, 2018
Published: October 23, 2018

DOI: 10.1021/acs.nanolett.8b02511
Nano Lett. 2018, 18, 6764−6769

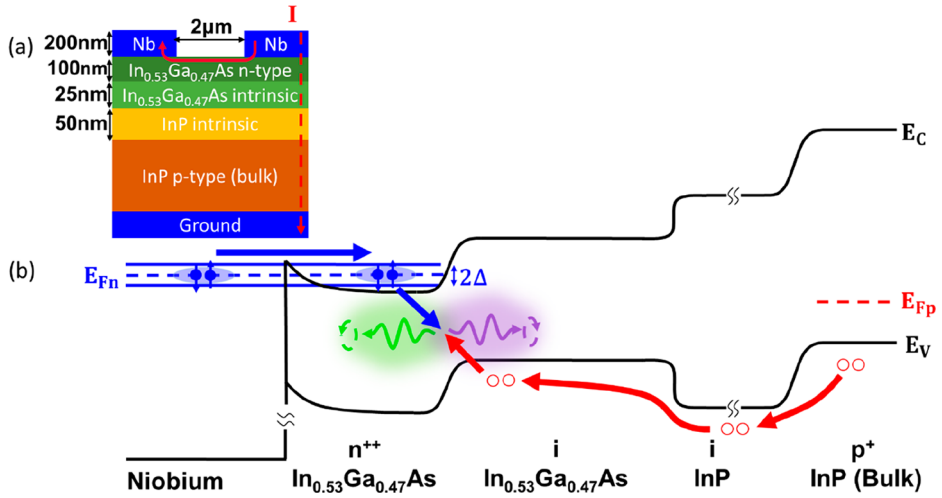

Figure 1. (a) SLED device structure showing layer thicknesses. Two measurement configurations are shown: (1) Top surface measurement (solid red arrow) in which current is injected between the two top contacts and which serves to test the existence of Andreev reflection in the device. (2) Junction measurement (dashed red arrow) in which current is injected into the PN junction resulting in emission. (b) Schematic drawing of SLED energy band structure under forward bias. Cooper-pairs are injected from the Nb contact into the heavily doped n-type $In_{0.53}Ga_{0.47}As$ layer and recombine with holes injected from the p-type InP substrate. The recombination occurs inside the $In_{0.53}Ga_{0.47}As$ which results in emission near 1.60 μm. Image not drawn to scale.

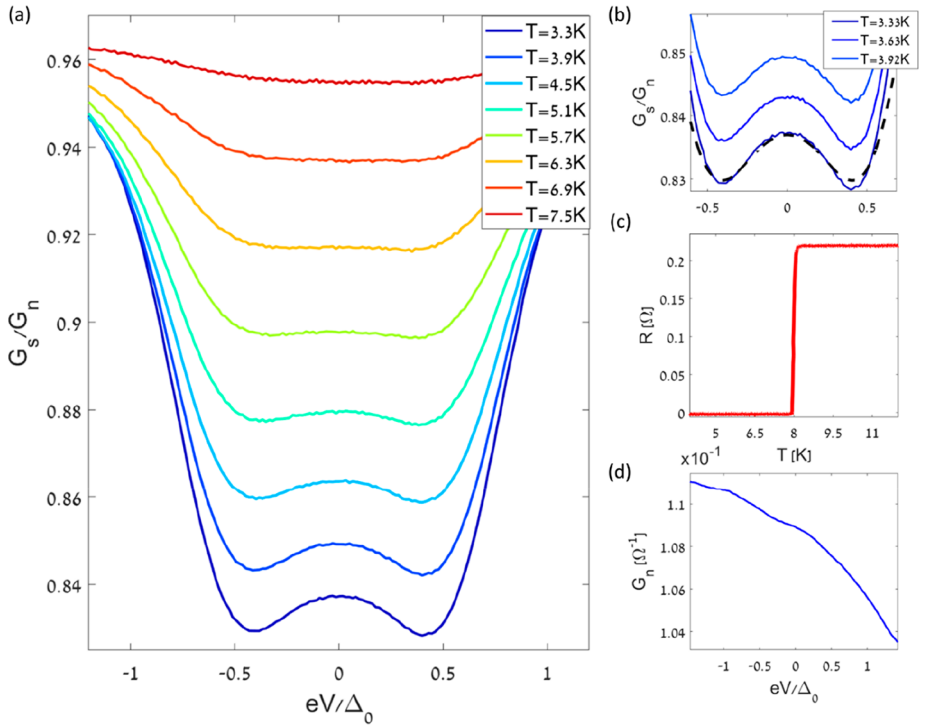

Figure 2. (a) Normalized differential conductance as a function of applied voltage in units of the Nb superconducting gap Δ_0 at T = 3.3 K. Conductance peak at zero voltage bias is prominent at low temperatures. (b) Low-temperature conductance spectrum presented in (a) showing enlarged central region along with the calculated curve (dashed black). (c) Resistance of the superconducting Nb contact as a function of temperature, exhibiting a transition temperature at 8 K. (d) Junction conductance spectrum above T_c which served for normalization.

ductor interface. This was made possible by a specially designed very low resistance superconductor−semiconductor interface, as well as large distance between superconducting pads, which are much larger than the coherence length. Therefore, no Josephson effects occur in our structure, allowing the observation of Andreev reflection. The electroluminescence spectrum of the SLED shows enhanced emission below T_c at the quasi-Fermi level in the conduction band, corresponding to the energy of the injected Cooper-pairs. Our theoretical models of both Andreev reflection and luminescence enhancement are in good agreement with the measurements. The SLED structure enabling both electroluminescence and Andreev reflection with challenging and contradicting requirements, was obtained by optimization of semiconductor layer doping and thicknesses. Since in superconductors Cooper pairs reside at the Fermi energy level, the semiconductor must be heavily doped to the point of degeneracy in order to realize Cooper-pair injection. Moreover, such heavy doping has the

DOI: 10.1021/acs.nanolett.8b02511
Nano Lett. 2018, 18, 6764−6769

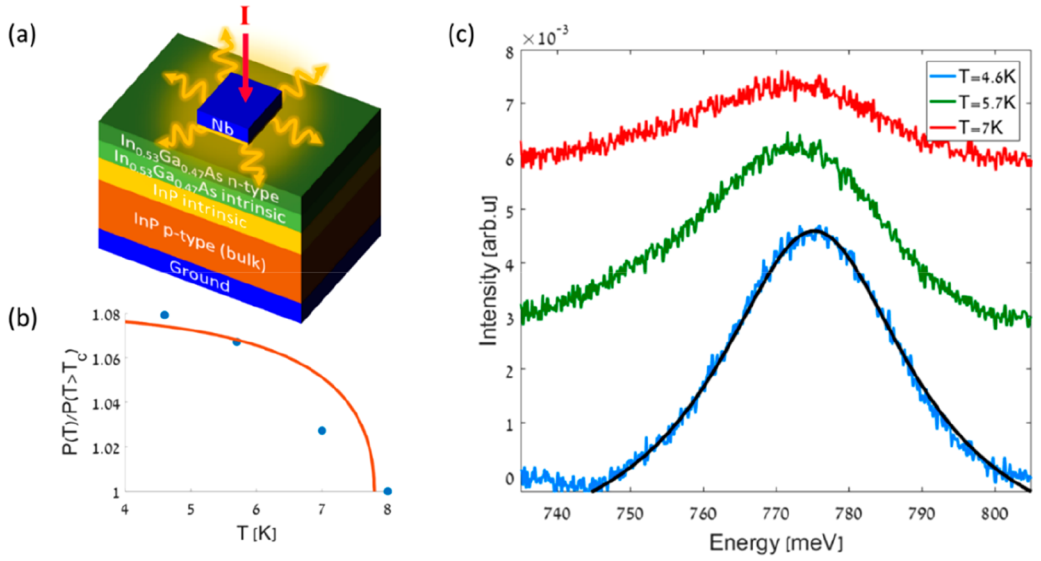

Figure 3. (a) SLED structure in EL emission configuration. Current is injected through the upper Nb electrode into the PN junction. Because of the opaqueness of the Nb contact, emission (wavy yellow lines) is only observed from the edges of the contact. (b) Measured (blue) normalized power (relative to emission power above T_c) vs temperature. The calculated curve (orange) is based on ref 12. (c) Spectrally resolved normalized electroluminescence measurements taken below T_c. The curves are shifted vertically for clarity. Emission enhancement is obtained in spectral range from 760 to 790 meV. Black line is the calculated spectrum.

advantage of reducing the thickness of the Schottky barrier which forms at the superconductor−semiconductor junctions.[22,29] On the other hand, heavy doping can reduce the efficiency of radiative recombination due to competing nonradiative processes such as Auger recombination.

The light-emitting structure with an active $In_{0.53}Ga_{0.47}As$ layer (Figure 1a) was grown on a p-type InP substrate by the metal organic molecular beam epitaxy (MOMBE) technique.[30] A 50 nm thick layer of intrinsic InP was grown on the InP substrate in order to serve as a buffer between the heavily doped substrate and the rest of the device. On top of the buffer layer, a 25 nm layer of intrinsic $In_{0.53}Ga_{0.47}As$ was grown, which serves as the active emitting region (an intrinsic layer is crucial as heavily doped layers suffer from reduced emission due to competing nonradiative processes). Finally, a 100 nm thick layer of Sn degenerately doped (5×10^{19} cm^{-3}) n-type $In_{0.53}Ga_{0.47}As$ terminates the undoped active layer in order to improve Cooper-pair injection efficiency into the LED. The semiconductor surface was Ar ion cleaned, and the 200 nm thick Nb superconducting contacts were deposited in situ using RF sputtering. Reactive ion etching (RIE) with lithography procedures formed the superconducting contacts with ∼100 μm × 100 μm area and ∼2 μm spacing, finalizing the device fabrication. The resulting Nb pad resistance was measured as a function of temperature in 4-probe configuration revealing a relatively high transition temperature (T_c) of 8 K (Figure 2c).

All the measurements were performed in liquid-He closed-cycle cryostat, using a lock-in amplifier to record differential conductance (dI/dV) spectra in a 4-probe configuration for various temperatures. The conductance measurements were performed in the in-plane configuration between the Nb pads and the InGaAs active layer (Figure 1a solid red arrow). The current bias for electroluminescence (EL) measurements was fed through the diode structure with contacts on top and bottom of the stack shown in Figure 1a (dashed red arrow). This configuration allows isolating the superconductor−semiconductor junction transport for Andreev reflection measurements. The device EL was modulated at a low frequency, spectrally resolved in a monochromator, and recorded in the lock-in detection scheme. A calibrated thermometer monitored the device temperature, and the current bias was kept at sufficiently low values to prevent the sample heating.

Our first experiments demonstrate the injection of Cooper pairs into the LED structure by Andreev reflection, crucial for utilization of superconductor properties such as spin-singlet electron pairing, which is a key ingredient for quantum light source realization. The differential conductance spectra measurements reveal the presence of Andreev reflection in the superconducting gap (Figure 2a,b), which results in a ZBCP at temperatures below superconducting transition temperature. The ZBCP appears on the background of a broader conductance minimum corresponding to quasiparticle tunneling. This complex conductance spectrum including both Andreev reflection and tunneling signatures has been observed previously in superconductor-normal junctions.[22,31] In conventional s-wave superconductors, the width of Andreev peak is determined by the superconducting gap width. In case of the proximity effect, induced by Cooper pair injection by Andreev reflection in to the normal material,[32] a smaller superconducting gap is induced in a thin layer of the normal material which determines the width of the Andreev conductance peak.[1] Therefore, the width of the smaller peak is determined by the induced smaller superconducting gap, as well as the effect of the broadening by temperature, disorder, and dephasing.

This spectral shape is attributed to the variation of contact quality along the superconducting−normal (S−N) interface with regions of low contact resistance contributing to the Andreev reflection signature (which is smaller as it is induced through the proximity effect) and high contact resistance regions contributing to the quasiparticle tunneling spectrum background. Both the Andreev ZBCP and the tunneling signatures disappear at temperatures approaching the superconductor critical temperature T_c (Figure 2a). The differential conductance spectra were normalized by the measurement

DOI: 10.1021/acs.nanolett.8b02511
Nano Lett. 2018, 18, 6764−6769

above the critical temperature (Figure 2d) to rule out any nonsuperconducting behavior of the device. Ideal low-temperature tunneling conductance should approach zero at energies below the gap. However, quasiparticle dephasing[39] and disorder[38] introduce significant broadening, which results in considerable conductance below the gap energies even at very low temperatures. The tunneling conductance through a high barrier in an ordered superconductor is typically characterized by an energy gap in the modified density of states as well as two peaks representing the long-range coherence.[33] Nevertheless, localization of the Cooper pairs due to disorder was predicted to result in a significant reduction of coherence, therefore leading to disappearance of coherence peaks in the conductance spectra.[34] These effects have been observed experimentally, exhibiting gapped conductance plots with reduced or disappearing coherence peaks in disordered superconductors.[35,36]

Therefore, the tunneling conductance dip without coherence peaks is attributed to the system disorder near the interface, resulting in Cooper pairs with reduced long-range coherence.

The second set of our experiments demonstrate enhanced electroluminescence below the superconducting transition from the active region of the SLED under forward current bias after removing high-temperature emission background. This radiative recombination process results in enhanced luminescence at temperatures below T_c and is spectrally centered around the quasi-Fermi energy level, where the superconducting gap is located. The electroluminescence spectrum at 4.6 K shows a clear maximum at the quasi-Fermi energy level, corresponding to the injected Cooper energy (Figure 3c). With increasing temperature, the luminescence enhancement reduces significantly, matching the calculated dependence (Figure 3b).

We modeled the differential conductance spectra in superconducting−normal (S−N) junction using the Blonder−Tinkham−Klapwijk (BTK) formalism,[21] assuming a delta-like potential barrier at the interface based on the Bogoliubov−de Gennes (BdG) equations,[37] which describe the transport across S−N interface

$$\left[-\frac{\hbar^2}{2m}\nabla^2 - \mu(x) + V(x)\right]u(x,t) + \Delta(x)v(x,t) = i\hbar\frac{\partial u(x,t)}{\partial t}$$

$$\left[\frac{\hbar^2}{2m}\nabla^2 + \mu(x) - V(x)\right]v(x,t) + \Delta(x)u(x,t) = i\hbar\frac{\partial v(x,t)}{\partial t} \quad (1)$$

where $u(x,t)$, $v(x,t)$ are the quasi-particle wave functions, $V(x)$ is a spatially dependent potential,$\Delta(x)$ is the superconducting gap, and $\mu(x)$ is the chemical potential. The wave function amplitudes together with the magnitude of the potential barrier are directly related to the conducance of the SN junction. According to the BTK model,[21] Andreev reflection and quasiparticle tunneling are competing processes which depend on barrier strength $Z = k_F H/2E_F$, where k_F and E_F are the Fermi wavenumber and energy respectively, and H is the potential barrier amplitude. Small barrier strength leads to Andreev reflection without quasiparticle tunneling spectra, while large barrier strength leads to quasiparticle tunneling spectral dip without an Andreev reflection feature. Because of the large area of our planar junctions, significantly larger than the coherence length of the superconductor, the low-resistance and high-resistance contact regions were modeled as parallel junctions with different barrier strength parameters Z. This approach has been used previously for large-area planar junctions resulting in good predictions to experimental results.[31] The lower-resistance junction has a smaller proximity-induced superconducting gap inside the semiconductor, resulting in Andreev reflection occurring not at the material interface but rather in the semiconductor between its normal and proximity regions with virtually zero Z parameter.[1] On the other hand, the high-resistance junction has a large Z parameter, explaining the quasiparticle tunneling spectral dip.

Each of the two junction types was modeled using the parameter set Δ_n, Γ_n, Z_n, γ_n, δ_n (Table 1). The superconducting gap of Nb without proximity effects is given by Δ_0, while the smaller proximity induced gap in the semiconductor in the low-resistance region is given by Δ_1. The calculation includes the spectral broadening due to temperature (γ_n) in the Fermi−Dirac distribution,[20] by Gaussian distribution of disorder (δ_n),[38] and quasiparticle dephasing[39] (Γ_n) (included as an imaginary energy term $E + i\Gamma_n$). The index n indicates the junction with $n = 0$ marking the high resistance junction and $n = 1$ indicates the low resistance junction. All parameters are given with respect to Δ_0. The calculated conductance spectra are in good agreement with the experimental results (Figure 2b) with extracted fit parameters given in Table 1.

Table 1. Parameters Used for the Theoretical Conductance Spectrum Curve Shown in Figure 2b (Dashed Line)[a]

parameter	Δ_0,Δ_1	Γ_0,Γ_1	Z_0,Z_1	γ_0,γ_1	δ_0,δ_1
value	Δ_0	$\Gamma_0 = 0.23\Delta_0$	$Z_0 = 1.5$	$\gamma_0 = 0.08\Delta_0$	$\delta_0 = 0.07\Delta_0$
	$\Delta_1 = 0.3\Delta_0$	$\Gamma_1 = 0.23\Delta_0$	$Z_1 = 0$	$\gamma_1 = 0.08\Delta_0$	$\delta_1 = 0.07\Delta_0$

[a]All parameters are given with respect to Δ_0.

The extracted value of thermal broadening agrees with the temperature of the experiment, while the disorder broadening is comparable to the typical disorder obtainable in epitaxial semiconductors structure growth.[38] The dephasing Γ_n was previously shown to be dominated by carrier−carrier scattering at low temperatures[40] and thus strongly dependent on carrier density. In our transport experiments, the low current (∼100 μA) results in low injected carrier density and correspondingly slow dephasing time (>1 ps), therefore making temperature, disorder, and dephasing broadening comparable in the conductance spectra. In our electroluminescence experiments, however, the relatively strong currents (∼10 mA) result in much faster carrier−carrier scattering induced dephasing times (<100 fs), thus making dephasing the dominant spectral broadening factor, while disorder and thermal broadening remain similar to those of the electrical transport experiment.

The theoretical modeling of the electroluminescence intensity spectra is based on the second-order perturbation calculation for Cooper-pair enhanced emission[11]

$$I(\omega_{q_u}^{ph}, \omega_{q_v}^{ph}) \propto \left|\frac{\Delta}{\Omega}\right|^2 \left(\frac{1}{(\omega_{q_u}^{ph} - \omega_{q_v}^{ph})^2 - \Omega^2} + \frac{1}{(\omega_{q_u}^{ph} - \omega_{q_v}^{ph} + \Omega)(\omega_{q_v}^{ph} - \omega_{q_u}^{ph} - \Omega)} + \frac{1}{(\omega_{q_v}^{ph} - \omega_{q_u}^{ph})^2 - \Omega^2} + \frac{1}{(\omega_{q_v}^{ph} - \omega_{q_u}^{ph} + \Omega)(\omega_{q_u}^{ph} - \omega_{q_v}^{ph} - \Omega)} \right) \quad (2)$$

DOI: 10.1021/acs.nanolett.8b02511
Nano Lett. 2018, 18, 6764−6769

where $\Omega = \sqrt{(\omega_{q_u}^{ph} + \omega_{q_v}^{ph} - 2\tilde{\mu}_n)^2 + 4\Delta^2}$, Δ is the superconducting gap parameter (with the assumption of being spatially independent), $\tilde{\mu}_n$ is the semiconductor Fermi energy level relative to the conduction band edge E_c, and sum of the photon pair energies $\omega_{qu}^{ph} + \omega_{qv}^{ph} \approx 2E_g$ where E_g is the semiconductor bandgap. Our model for EL is based on Fermi Golden rule calculation of emission rates based on carrier injection into semiconductors, similar to regular one-photon emission done by first-order perturbation[41] but using second-order perturbation in our case due to Cooper pair decay effect.[9] The dephasing, disorder, and the thermal broadening affect EL spectra, similar to the effect on electrical transport in principle. However, higher carrier densities and corresponding short dephasing times shorter than 100 fs result in dephasing being the dominant broadening effect for EL spectra. The corresponding spectral broadening is an order of magnitude larger than the superconducting gap in our experiment, making it impossible to resolve the superconducting gap structure in the luminescence spectra under such strong currents. The shape of the calculated spectrum (Figure 3c black curve) agrees well with that of the measured one, whereas the magnitude of the calculated maximum is a fit to the experimental data. Moreover, the integrated intensity has also been calculated (Figure 3 b). The measured emission power versus temperature (circles in Figure 3b) with the calculated dependence shown by the solid line, reaches a value of ∼8% enhancement at T = 4 K, relative to the emission above T_c. The relatively small enhancement can be attributed to the fact that current is injected into the semiconductor structure not only as Cooper pairs (seen in Andreev reflection in Figure 2) but also as single quasiparticles (seen as the tunneling part of the spectra in Figure 2). Above T_c, no enhancement was observed. The emission efficiency (emitted photons per injected carrier) of our SLED device is estimated to be ∼0.01% with emission rate of $\sim 10^{12}$ photons/s, which can be further enhanced in future devices by carrier injection and light extraction optimization. In comparison, the highest reported efficiency (emitted photons per pump photon) for conventional methods such as spontaneous parametric down conversion[42] is $\sim 10^{-4}$% with corresponding emission rate on the order of $\sim 10^7$ photons/s.

The devices in our experiment, as well as in previous works,[7,23,24] are based on narrow-bandgap materials such as InGaAs, which enable efficient Cooper pair injection due to the relatively small Schottky barrier at the interface with the superconducting contact. However, narrow-bandgap devices emit photons in the long wavelength range, which makes single-photon counting and correlations challenging. On the other hand, wider-bandgap materials emitting in the Si photon counter wavelength range such as AlGaAs, suitable for photon correlation experiments, make Cooper pair injection difficult due to higher Schottky barriers. A promising solution to this trade-off was proposed based on resonant tunneling of Cooper pairs into AlGaAs structures despite higher barriers,[43] enabling future photon correlation experiments. Another interesting direction for future SLED studies can be applying magnetic fields, resulting in effects such as reflectionless tunneling.[44] However, this involves challenges of cryogenic environments with both optical access as well as relatively strong magnetic fields.

In conclusion, we demonstrated Cooper-pair injection into a superconducting light-emitting structure by performing differential conductance spectroscopy, which reveals Andreev reflection at the superconductor−semiconductor interface. We show enhanced electroluminescence from the device below T_c at the quasi-Fermi level. The calculated conductance and electroluminescence spectra based on Cooper-pair injection into the semiconductor correspond well to our experimental results. Our findings enable future superconductor−semiconductor quantum optoelectronics devices.

AUTHOR INFORMATION

ORCID

Krishna Balasubramanian: 0000-0001-6307-7425

Alex Hayat: 0000-0002-6579-7431

Notes

The authors declare no competing financial interest.

ACKNOWLEDGMENTS

This research was supported by the ISF-NSFC joint research program (Grant 2220/15) and ISF FIRST Program (Grant 1995/17).

REFERENCES

(1) Nishino, T.; Hatano, M.; Hasegawa, H.; Kure, T.; Murai, F. Carrier reflection at the superconductor-semiconductor boundary observed using a coplanar-point-contact injector. *Phys. Rev. B: Condens. Matter Mater. Phys.* **1990**, *41*, 7274−7276.

(2) Heslinga, D. R.; Shafranjuk, S. E.; Van Kempen, H.; Klapwijk, T. M. Observation of double-gap-edge Andreev reflection at Si/Nb interfaces by point-contact spectroscopy. *Phys. Rev. B: Condens. Matter Mater. Phys.* **1994**, *49*, 10484−10494.

(3) Mou, S. S.; Irie, H.; Asano, Y.; Akahane, K.; Kurosawa, H.; Nakajima, H.; Kumano, H.; Sasaki, M.; Suemune, I. Superconducting light-emitting diodes. *IEEE J. Sel. Top. Quantum Electron.* **2015**, *21*, 1−11.

(4) Mou, S. S.; Irie, H.; Asano, Y.; Akahane, K.; Kurosawa, H.; Nakajima, H.; Kumano, H.; Sasaki, M.; Suemune, I. Optical observation of superconducting density of states in luminescence spectra of InAs quantum dots. *Phys. Rev. B: Condens. Matter Mater. Phys.* **2015**, *92*, 035308.

(5) Suemune, I.; Akazaki, T.; Tanaka, K.; Jo, M.; Uesugi, K.; Endo, M.; Kumano, H.; Hanamura, E.; Takayanagi, H.; Yamanishi, M.; Kan, H. Superconductor-based quantum-dot light-emitting diodes: role of Cooper pairs in generating entangled photon pairs. *Jpn. J. Appl. Phys.* **2006**, *45*, 9264−9271.

(6) Khoshnegar, M.; Majedi, A. H. Entangled photon pair generation in hybrid superconductor−semiconductor quantum dot devices. *Phys. Rev. B: Condens. Matter Mater. Phys.* **2011**, *84*, 104504.

(7) Suemune, I.; Hayashi, Y.; Kuramitsu, S.; Tanaka, K.; Akazaki, T.; Sasakura, H.; Inoue, R.; Takayanagi, H.; Asano, Y.; Hanamura, E.; Odashima, S. A. Cooper-pair light-emitting diode: Temperature dependence of both quantum efficiency and radiative recombination lifetime. *Appl. Phys. Express* **2010**, *3*, 054001.

(8) Sabag, E.; Bouscher, S.; Marjieh, R.; Hayat, A. Photonic Bell-state analysis based on semiconductor-superconductor structures. *Phys. Rev. B: Condens. Matter Mater. Phys.* **2017**, *95*, 094503.

(9) Marjieh, R.; Sabag, E.; Hayat, A. Light Amplification in Semiconductor-Superconductor Structures. *New J. Phys.* **2016**, *18*, 023019.

(10) Inoue, R.; Takayanagi, H.; Akazaki, T.; Tanaka, K.; Sasakura, H.; Suemune, I. Carrier flow and nonequilibrium superconductivity in superconductor-based LEDs. *Appl. Phys. Express* **2014**, *7*, 073101.

(11) Hayat, A.; Kee, H. Y.; Burch, K. S.; Steinberg, A. M. Cooper-pair-based photon entanglement without isolated emitters. *Phys. Rev. B: Condens. Matter Mater. Phys.* **2014**, *89*, 94508.

(12) Asano, Y.; Suemune, I.; Takayanagi, H.; Hanamura, E. Luminescence of a Cooper Pair. *Phys. Rev. Lett.* **2009**, *103*, 187001.

DOI: 10.1021/acs.nanolett.8b02511
Nano Lett. 2018, 18, 6764−6769

(13) Akopian, N.; Lindner, N. H.; Poem, E.; Berlatzky, Y.; Avron, J.; Gershoni, D.; Gerardot, B. D.; Petroff, P. M. Entangled photon pairs from semiconductor quantum dots. *Phys. Rev. Lett.* **2006**, *96*, 130501.
(14) Hayat, A.; Ginzburg, P.; Orenstein, M. Observation of two-photon emission from semiconductors. *Nat. Photonics* **2008**, *2*, 238−241.
(15) Hayat, A.; Ginzburg, P.; Orenstein, M. Measurement and model of the infrared two-photon emission spectrum of GaAs. *Phys. Rev. Lett.* **2009**, *103*, 023601.
(16) Hayat, A.; Ginzburg, P.; Orenstein, M. High-rate entanglement source via two-photon emission from semiconductor quantum wells. *Phys. Rev. B: Condens. Matter Mater. Phys.* **2007**, *76*, 035339.
(17) Lin, Z.; Vučković, J. Enhanced two-photon processes in single quantum dots inside photonic crystal nanocavities. *Phys. Rev. B: Condens. Matter Mater. Phys.* **2010**, *81*, 035301.
(18) Nevet, A.; Berkovitch, N.; Hayat, A.; Ginzburg, P.; Ginzach, S.; Sorias, O.; Orenstein, M. Plasmonic nanoantennas for broad-band enhancement of two-photon emission from semiconductors. *Nano Lett.* **2010**, *10*, 1848−1852.
(19) Ota, Y.; Iwamoto, S.; Kumagai, N.; Arakawa, Y. Spontaneous two-photon emission from a single quantum dot. *Phys. Rev. Lett.* **2011**, *107*, 233602.
(20) Tinkham, M. *Introduction to superconductivity*; McGraw-Hill, 1996.
(21) Blonder, G. E.; Tinkham, M.; Klapwijk, T. M. Transition from metallic to tunneling regimes in superconducting microconstrictions: Excess current, charge imbalance, and supercurrent conversion. *Phys. Rev. B: Condens. Matter Mater. Phys.* **1982**, *25*, 4515−4532.
(22) Kastalsky, A.; Kleinsasser, A. W.; Greene, L. H.; Bhat, R.; Milliken, F. P.; Harbison, J. P. Observation of pair currents in superconductor-semiconductor contacts. *Phys. Rev. Lett.* **1991**, *67*, 3026−3029.
(23) Takayanagi, H.; Inoue, R.; Akazaki, T.; Tanaka, K.; Suemune, I. Superconducting transport in an LED with Nb electrodes. *Phys. C* **2010**, *470*, 814−817.
(24) Inoue, R.; Takayanagi, H.; Akazaki, T.; Tanaka, K.; Suemune, I. Transport characteristics of a superconductor-based LED. *Supercond. Sci. Technol.* **2010**, *23*, 034025.
(25) Recher, P.; Nazarov, Y. V.; Kouwenhoven, L. P. Josephson Light-Emitting Diode. *Phys. Rev. Lett.* **2010**, *104*, 156802.
(26) Godschalk, F.; Hassler, F.; Nazarov, Y. V. Proposal for an optical laser producing light at half the Josephson frequency. *Phys. Rev. Lett.* **2011**, *107*, 073901.
(27) Hassler, F.; Nazarov, Y. V.; Kouwenhoven, L. P. Quantum manipulation in a Josephson light-emitting diode. *Nanotechnology* **2010**, *21*, 274004.
(28) Godschalk, F.; Nazarov, Y. V. Light-superconducting interference devices. *Phys. Rev. B: Condens. Matter Mater. Phys.* **2014**, *89*, 104502.
(29) Pierret, R. F. *Semiconductor device fundamentals*; Pearson Education India, 1996.
(30) Hamm, R. A.; Ritter, D.; Temkin, H. Compact metalorganic molecular-beam epitaxy growth system. *J. Vac. Sci. Technol., A* **1994**, *12*, 2790−2794.
(31) Zareapour, P.; Hayat, A.; Zhao, S. Y. F.; Kreshchuk, M.; Jain, A.; Kwok, D. C.; Lee, N.; Cheong, S. W.; Xu, Z.; Yang, A.; Gu, G. D.; et al. Proximity-induced high-temperature superconductivity in the topological insulators Bi_2Se_3 and Bi_2Te_3. *Nat. Commun.* **2012**, *3*, 1056.
(32) Pannetier, B.; Courtois, H. Andreev reflection and proximity effect. *J. Low Temp. Phys.* **2000**, *118*, 599−615.
(33) Sacépé, B.; Dubouchet, T.; Chapelier, C.; Sanquer, M.; Ovadia, M.; Shahar, D.; Feigel'man, M.; Ioffe, L. Localization of preformed Cooper pairs in disordered superconductors. *Nat. Phys.* **2011**, *7*, 239−244.
(34) Bouadim, K.; Loh, Y. L.; Randeria, M.; Trivedi, N. Single-and two-particle energy gaps across the disorder-driven superconductor−insulator transition. *Nat. Phys.* **2011**, *7*, 884−889.
(35) Kamlapure, A.; Das, T.; Ganguli, S. C.; Parmar, J. B.; Bhattacharyya, S.; Raychaudhuri, P. Emergence of nanoscale inhomogeneity in the superconducting state of a homogeneously disordered conventional superconductor. *Sci. Rep.* **2013**, *3*, 2979.
(36) Panna, D.; Balasubramanian, K.; Bouscher, S.; Wang, Y.; Yu, P.; Chen, X.; Hayat, A. Nanoscale High-Tc YBCO/GaN super-Schottky diode. *Sci. Rep.* **2018**, *8*, 5597.
(37) Bardeen, J.; Cooper, L. N.; Schrieffer, J. R. Microscopic theory of superconductivity. *Phys. Rev.* **1957**, *106*, 162−164.
(38) Herman, M. A.; Bimberg, D.; Christen, J. Heterointerfaces in quantum wells and epitaxial growth processes: Evaluation by luminescence techniques. *J. Appl. Phys.* **1991**, *70*, R1−R52.
(39) Dynes, R. C.; Narayanamurti, V.; Garno, J. P. Direct measurement of quasiparticle-lifetime broadening in a strong-coupled superconductor. *Phys. Rev. Lett.* **1978**, *41*, 1509−1512.
(40) Snoke, D. W. Density dependence of electron scattering at low density. *Phys. Rev. B: Condens. Matter Mater. Phys.* **1994**, *50*, 11583−11591.
(41) Coldren, L. A.; *Diode Lasers and Photonic Integrated Circuits*, 2nd ed.; John Wiley & Sons, 1995.
(42) Bock, M.; Lenhard, A.; Chunnilall, C.; Becher, C. Highly efficient heralded single-photon source for telecom wavelengths based on a PPLN waveguide. *Opt. Express* **2016**, *24*, 23992−24001.
(43) Bouscher, S.; Winik, R.; Hayat, A. Andreev reflection enhancement in semiconductor-superconductor structures. *Phys. Rev. B: Condens. Matter Mater. Phys.* **2018**, *97*, 054512.
(44) Van Wees, B. J.; De Vries, P.; Magnée, P.; Klapwijk, T. M. Excess conductance of superconductor-semiconductor interfaces due to phase conjugation between electrons and holes. *Phys. Rev. Lett.* **1992**, *69*, 510−513.

DOI: 10.1021/acs.nanolett.8b02511
Nano Lett. 2018, 18, 6764−6769